

Sensorless Direct Torque Control of Induction Motor Drive with LC Filter

Jaroslaw Guzinski

Gdansk University of Technology, Gdansk, Poland, jarguz@pg.gda.pl

Abstract — This paper focuses on some aspects of control and estimation problems for speed sensorless induction motor drive with inverter output LC. The filters are needed in some industrial drives with pulse width modulated (PWM) inverters. They smoothen the motor supply voltage and current so that nearly sinusoidal shapes are obtained. The filters can also limit the bearing current and shaft voltages. Because of the voltage drop and phase shift imposed by the filter, the motor voltages and currents differ from the inverter output. This fact can seriously complicate the drive operation due to the problems with the control and estimation process – especially in speed sensorless drives. To solve those problems the filter model should be taken into account in the control and estimation algorithms.

In this paper a sensorless solution for induction motor (IM) with inverter output filter drives is proposed. The new contribution of the paper is the application of the solution to direct torque control. A short description and discussion of the schemes is given. Simulation and experimental results validate the proposed solution.

Keywords — Direct torque control, Inverter output filter, Sensorless control, High performance drives.

I. INTRODUCTION

In nowadays adjustable speed drives (ASD) the most available drive systems are with induction motor and voltage inverter type supply. Inverter output voltage is generated by pulse width modulation (PWM) algorithm. Due to high dv/dt the inverter gives some unwanted effects such as bearing currents, shaft voltages, insulation stress, efficiency decrease, noises etc. [1], [2]. The problems are underlined in case of long cable connection. Listened ASD drawbacks could be reduced if passive filter is installed on the inverter output [3] – Fig. 1.

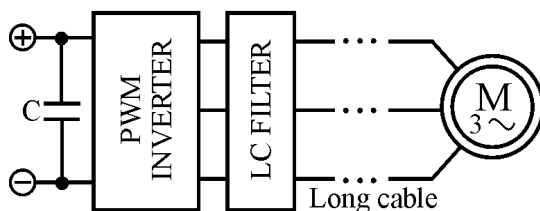


Fig. 1. Induction motor variable speed drive with inverter output filter.

With LC filer the motor supply voltage is close to sinusoidal shape – Fig. 2. The design process of the LC filter requires obtaining voltage THD less than 5% – according to IEEE 519-1992 standards [4].

The use of LC filter cause various problems for the control and estimation systems. The reason is that the actual motor voltages and currents differ from measured

by the inverter sensors. For system simplicity if the filter is installed additional voltage and currents sensors are not recommended. Furthermore, the speed sensor is eliminated in most of ASD. Therefore, the LC filter installation in the drive requires modifications in the control and estimation algorithms [5], [6].

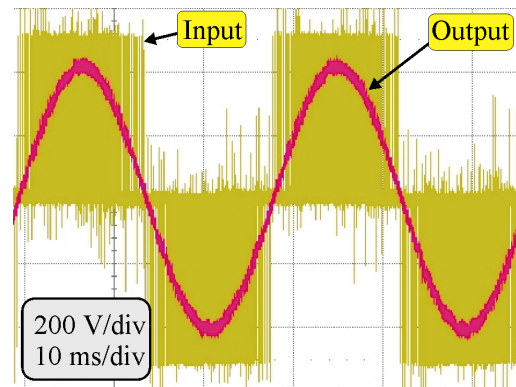


Fig. 2. LC filter input-output voltage - motor supply is sinusoidal.

In ASD with filters only the solutions for field oriented control (FOC) [5], [7], nonlinear FOC [10] and multiscalar control [8], [9] were presented – to the knowledge of the author no such work is devoted to direct torque control (DTC).

This paper presents sensorless DTC method for induction motor with voltage source inverter and LC filter. The DTC with PWM is used for motor control whereas the multiloop LC filter control is subordinated. The Luenberger based flux and speed observer with motor and filter models equations is used. the only used sensors in the drive system are dc link voltage and inverter output currents.

II. SYSTEM MODEL

A. Model of LC filter

The LC filter has a structure presented in Fig. 3. Three chokes L_1 and capacitors C_1 are parts of the low pass filter. Resistor R_C is used for transients damping.

The equations of the filter for the ABC frame related to the dc link negative terminal (C_{DC}) are transformed into $\alpha\beta$ orthogonal frame of reference (Fig. 4) [10]:

$$\begin{bmatrix} u_{1\alpha} \\ u_{1\beta} \end{bmatrix} = L_1 \frac{d}{d\tau} \begin{bmatrix} i_{1\alpha} \\ i_{1\beta} \end{bmatrix} + \begin{bmatrix} u_{sa} \\ u_{s\beta} \end{bmatrix} \quad (1)$$

$$\begin{bmatrix} u_{sa} \\ u_{s\beta} \end{bmatrix} = \begin{bmatrix} u_{ca} \\ u_{c\beta} \end{bmatrix} + R_c \begin{bmatrix} i_{ca} \\ i_{c\beta} \end{bmatrix} \quad (2)$$

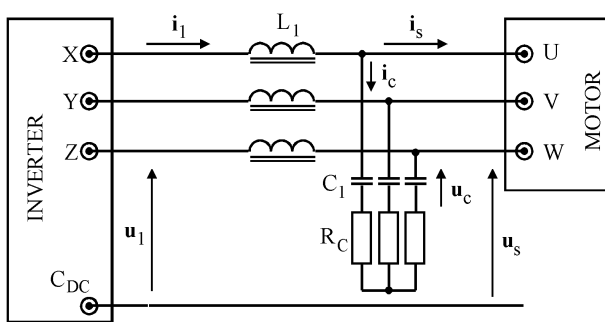


Fig. 3. Structure of the inverter output filter.

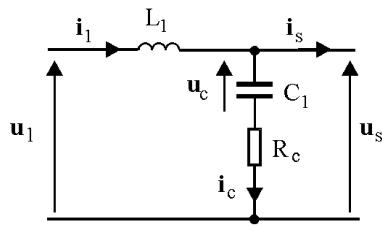


Fig. 4. Electrical circuit of LC filter in $\alpha\beta$ references.

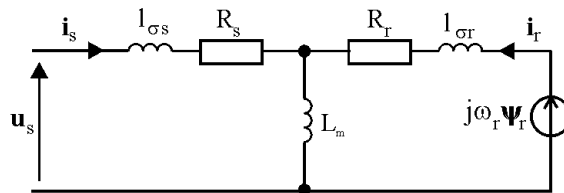


Fig. 5. Electrical circuit of induction motor in $\alpha\beta$ references.

$$C_1 \frac{d}{d\tau} \begin{bmatrix} u_{ca} \\ u_{cb} \end{bmatrix} = \begin{bmatrix} i_{1a} \\ i_{1b} \end{bmatrix} - \begin{bmatrix} i_{sa} \\ i_{sb} \end{bmatrix} \quad (3)$$

$$\begin{bmatrix} i_{1a} \\ i_{1b} \end{bmatrix} = \begin{bmatrix} i_{sa} \\ i_{sb} \end{bmatrix} + \begin{bmatrix} i_{ca} \\ i_{cb} \end{bmatrix} \quad (4)$$

where τ is time per unit, i.e., $\tau=2\pi f_0 t$, and f_0 is the electrical grid frequency.

The filter electrical circuits in $\alpha\beta$ is presented in Fig. 4.

B. Model of induction motor

The IM model in per unit system is [10]:

$$\frac{d}{d\tau} \begin{bmatrix} i_{sa} \\ i_{sb} \end{bmatrix} = a_1 \begin{bmatrix} i_{sa} \\ i_{sb} \end{bmatrix} + a_2 \begin{bmatrix} \Psi_{ra} \\ \Psi_{rb} \end{bmatrix} + a_3 \omega_r \begin{bmatrix} \Psi_{rb} \\ -\Psi_{ra} \end{bmatrix} + a_4 \begin{bmatrix} u_{sa} \\ u_{sb} \end{bmatrix} \quad (5)$$

$$\frac{d}{d\tau} \begin{bmatrix} \Psi_{ra} \\ \Psi_{rb} \end{bmatrix} = a_5 \begin{bmatrix} \Psi_{ra} \\ \Psi_{rb} \end{bmatrix} + \omega_r \begin{bmatrix} -\Psi_{rb} \\ \Psi_{ra} \end{bmatrix} + a_6 \begin{bmatrix} i_{sa} \\ i_{sb} \end{bmatrix} \quad (6)$$

$$\frac{d\omega_r}{d\tau} = \frac{1}{J} \left(\frac{L_m}{L_r} (\Psi_{ra} i_{sb} - \Psi_{rb} i_{sa}) - t_L \right) \quad (7)$$

where: t_L is load torque, J is motor inertia, and

$$\begin{aligned} a_1 &= -(R_s L_r^2 + R_r L_m^2) / (L_r w_\sigma), & a_2 &= R_r L_m / (L_r w_\sigma), \\ a_3 &= L_m / w_\sigma, & a_4 &= L_r / w_\sigma, & a_5 &= -R_r / L_r, \\ a_6 &= R_r L_m / L_r \text{ and } w_\sigma = L_r L_s - L_m^2. \end{aligned}$$

III. CONTROL SYSTEM

Fig. 6 shows a block diagram of the control system. The main loops are for the motor control, whereas subordinate loops are for the filter control. The control system operates in synchronous dq coordinates – oriented with stator flux position

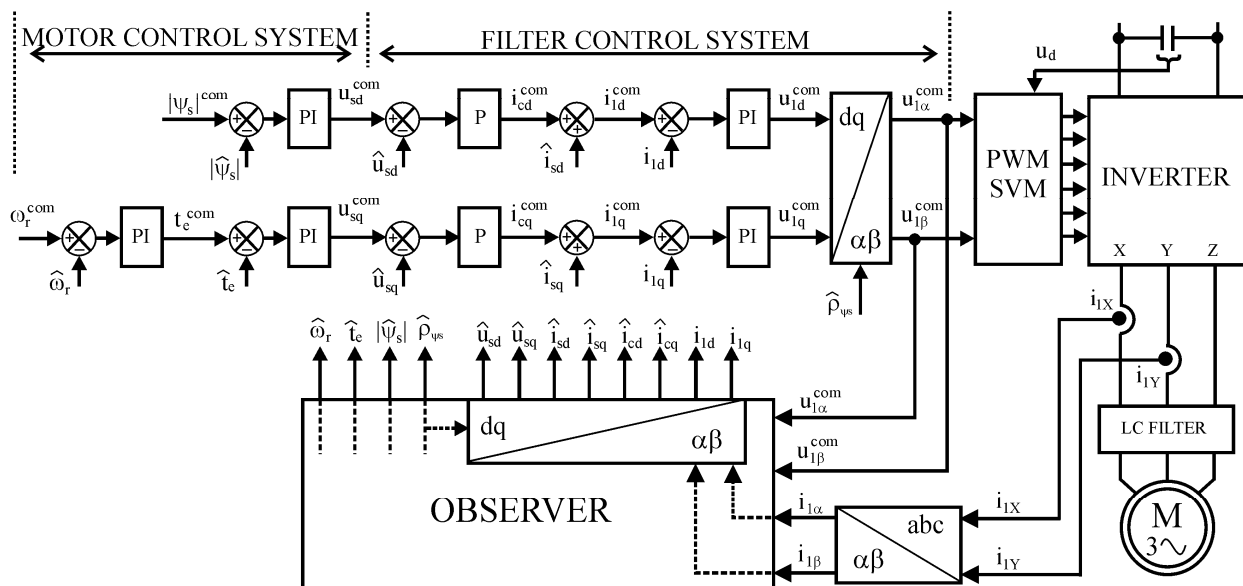


Fig. 6. Block diagram of DTC-SVM control for IM drive with LC filter (dq components are stator flux oriented, $\alpha\beta$ are stationary coordinates). Variables calculated in observer block are marked with ^ dash.

A. Motor control

Motor control is based on direct torque control (DTC) principle. The DTC idea is well known from 80s [11], [12]. The general principle is simple and interesting especially due to excellent torque dynamics. Because of some disadvantages, e.g. starting, low speed problems, torque ripple etc., the DTC is still under development [13], [25].

The main disadvantage of DTC is variable switching frequency which is depended on flux and torque hysteresis controller band. To eliminate this problem the classical voltage switching table is replaced by pulse width modulator (PWM) [14], [15]. With PWM modulator the torque and flux are forced by selection of the proper voltage vector generated in PWM algorithm. Because digital control of PWM modulator is mostly done due to space vector modulation (SVM) algorithm that type of constant switching DTC is named as DTC-SVM [16], [17].

In block scheme (Fig. 6) two PI controllers are used for flux magnitude $|\Psi_s|^{com}$ and torque t_e^{com} force. The output signals of the controllers are interpreted as commanded voltage components u_{sd}^{com} and u_{sq}^{com} where dq coordinates are stator flux oriented [26]. The control idea is to use stator simplified model [13]:

$$u_{sd} = R_s i_{sd} + d|\Psi_s|^{com} / dt \approx d|\Psi_s|^{com} / dt \quad (8)$$

$$u_{sq} = R_s i_{sq} + \omega_{\Psi s} |\Psi_s|^{com} = k_s t_e^{com} + \omega_{\Psi s} |\Psi_s|^{com} \quad (9)$$

where $\omega_{\Psi s}$ is stator flux vector angular speed and $k_s = R_s / |\Psi_s|^{com}$.

It can be noticed in (8) and (9) that u_{sd} has influence on $|\Psi_s|$ only and u_{sq} on torque control if $\omega_{\Psi s} |\Psi_s|$ term is decoupled [13]. To simplify the control also the decoupling term is sometimes omitted [26].

The commanded torque t_e^{com} is set by PI speed controller.

The DTC-SVM control structure is similar to the classical FOC control [25]. The main difference is that DTC-SVM has less controllers i.e. three instead of four used in FOC. Additionally in DTC-SVM no coordinate transformation for stator currents is required.

B. Filter control

The components of commanded motor voltage u_{sd}^{com} and u_{sq}^{com} would not be generated at the motor terminal because LC filter is installed. So additional control loops are applied – multiloop control. The task for the multiloop is to achieve the required motor voltage with simultaneous control of inverter output current. Such regulation is widely implemented in the uninterruptible power supply (UPS) [18]. This kind of regulation is also applicable in ASD [19].

As was presented in [20] the good properties are obtained with filter multiloop control when inverter current is used in feedback and motor current is used for disturbance compensation.

In the control structure in Fig. 6 the filter control part has outer voltage loop and inner current loop. The voltage controller is simple P-regulator. The P controller is sufficient due to the integration properties of the capacitor C_1 [21]. The u_s regulators create a reference signal of capacitor current i_c^{com} . Next i_s is added to i_c^{com}

and finally the commanded inverter current i_1^{com} is created. Use of i_s in feedback is for disturbance decoupling [22].

Current i_1 is controlled by PI type regulator – the regulators output is inverter output voltage u_1^{com} in dq which is next transformed to $\alpha\beta$ coordinates. Reference $u_{1\alpha\beta}^{com}$ is provided to PWM controller.

The obtained control structure is more complex in compare to DTC PWM without filter – 7 controllers versus 3. However additional controllers are necessary to perform full control of LC filter. The advantage of such complex system is that current is under control. It is worth to see that in classical DTC or DTC-SVM the current is beyond of control so additional blocks are required to protect the drive. That current protection is included in system showed in Fig. 6.

IV. OBSERVER

In the proposed drive, the sensors are limited to DC link voltage and inverter output currents. Other needed variables are estimated in the observer system which was proposed earlier by the author in [23].

The main idea of the estimation is from [24]. The idea is to extend Luenberger type estimator with redundant equations for motor electromotive force (EMF):

$$\begin{aligned} \xi_\alpha &= \Psi_{r\alpha} \omega_r \\ \xi_\beta &= \Psi_{r\beta} \omega_r \end{aligned} \quad (10)$$

The author has used this observer for both motor and filter estimation – the filter model was combined with the motor observer. Instead of using motor stator current in observer feedback channel the inverter output current was used.

Based on the estimated rotor flux and EMF the motor speed is taken from:

$$\hat{\omega}_r = (\hat{\xi}_\alpha \hat{\Psi}_{r\alpha} + \hat{\xi}_\beta \hat{\Psi}_{r\beta}) / \hat{\Psi}_r^2 \quad (11)$$

More details on the observer could be find in [23].

V SIMULATION AND EXPERIMENTS

A. Simulation results

For system investigation an ac drive with 3 kW was chosen, which is the same motor used in the experiments. The motor and filter data are given in Table I.

TABLE I
SPECIFICATION OF THE INDUCTION MOTOR AND LC FILTER

| Parameter | Value | Description |
|-----------|----------|---------------------------|
| P_N | 3 kW | rated power |
| U_N | 380 V | rated voltage |
| I_N | 6.4 A | rated current |
| f_N | 50 Hz | rated frequency |
| n_n | 1420 rpm | rated speed |
| $2p$ | 4 | poles |
| R_s | 1.9 Ω | stator resistance |
| R_r | 2.6 Ω | rotor resistance |
| L_m | 237 mH | mutual inductance |
| L_s | 244 mH | stator inductance |
| L_r | 244 mH | rotor inductance |
| L_f | 9 mH | filter inductance |
| C_1 | 8 μF | filter capacitance |
| R_C | 2.2 Ω | filter damping resistance |

The results are shown in per unit system – base values are given in Table II.

TABLE II
PER UNIT SYSTEM

| Definition | Description |
|----------------------------|-----------------------|
| $U_b=U_N$ | base voltage |
| $I_b=1.73*I_N$ | base current |
| $Z_b=U_b / I_b$ | base impedance |
| $T_b=(U_b I_b p)/\omega_0$ | base torque |
| $\Psi_b=U_b/\omega_0$ | base flux |
| $\Omega_b=\omega_0/p$ | base mechanical speed |
| $L_b=\Psi_b/I_b$ | base inductance |
| $\tau=\omega_0 t$ | relative time |

$$\text{where } \omega_0=2\pi f_N.$$

Examples of the simulation investigations for the full sensorless control system are presented in Fig. 7-9.

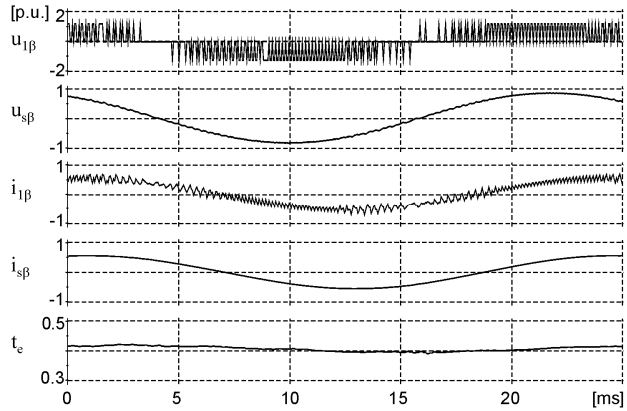


Fig. 7. Sensorless steady state operation (load torque $t_L=0.41$ p.u.)

Figure 7 presents steady state operation for $t_L=0.41$ p.u. It is shown that the PWM inverter output voltage has been converted into sinusoidal waveforms. The smoothed current is also observable. The motor torque maintains constant with variations less than 0.02 p.u.

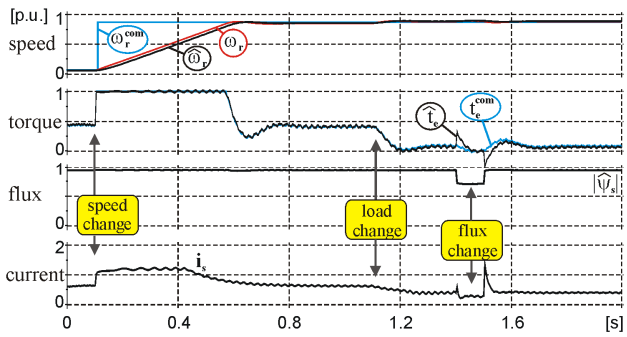


Fig. 8. Simulation results of the sensorless drive under speed, load and flux variation.

In Fig. 8 test the motor commanded speed was first changed, next the load torque was decreased and finally the motor flux was decreased and then increased.

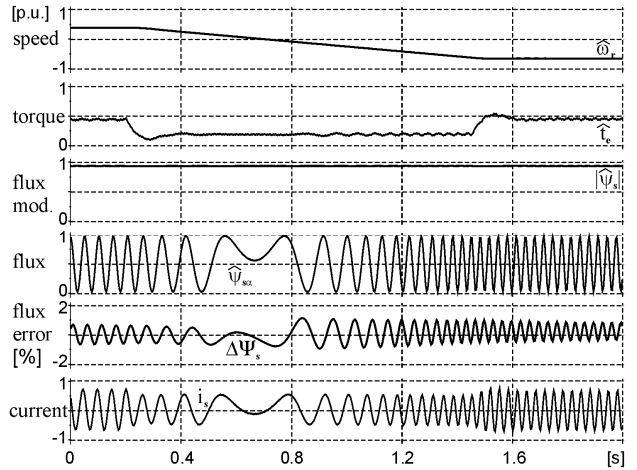


Fig. 9. Simulation results of the sensorless drive slow reverse (active load).

In Fig. 9 the motor slow reverse is presented. Constant load was used – load torque was not changed during reverse.

From the results it is noticeable that the drive is working properly. The controlled variables follow the commanded ones. The estimated and actual speeds match but with small error during transients. The motor flux estimation error is close to 1% - even when motor speed crosses zero value.

B. Laboratory set-up

The photos and structure of the laboratory set-up are presented in Fig. 10 and Fig. 11.

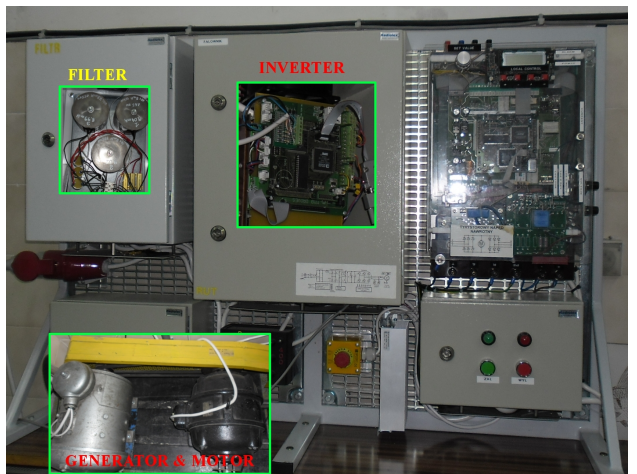


Fig. 10. Photos of the laboratory set-up elements.

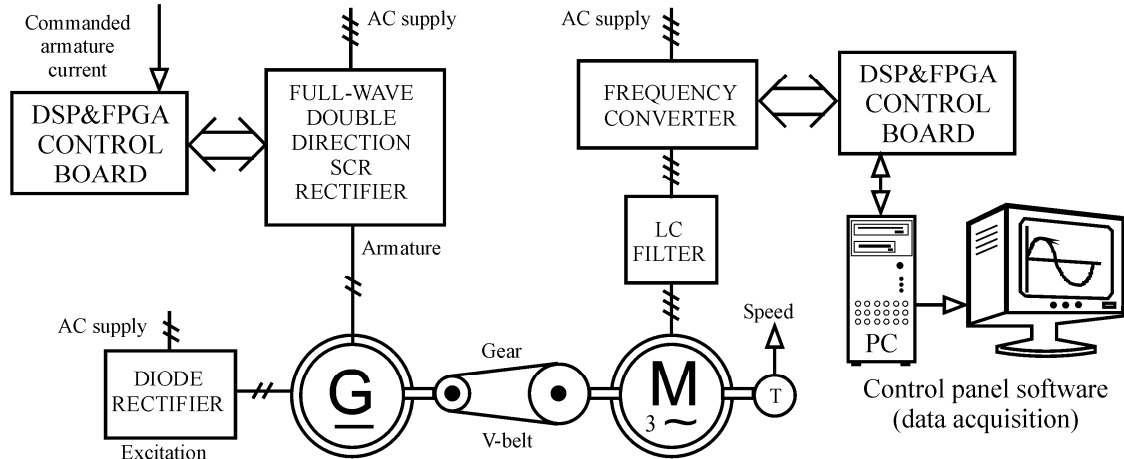


Fig. 11. Structure of the laboratory set-up (speed sensor is only for data acquisition – not used in control process).

The 3kW induction motor was coupled with a 5.5 kW DC machine. A gear with V-belts was used to match the machines speed – DC machine speed is 3000 rpm. The IM motor was supplied from voltage inverter. For DC machine the bi-directional rectifier with thyristors was used. For each of the converters separated DSP&FPGA control boards were used. Control board for an AC machine was connected to the PC thorough a serial link. The control panel software in PC was used to download the C-code to the DSP and to command the values as well as for data acquisition purposes. For DC machine an algorithm of armature current regulation was applied. Commanded armature current was set by the operator. The speed sensor for IM was installed but speed was not used in control process.

C. Experiments

Examples of the experimental results are presented in Fig. 12 – Fig. 14.

D. Robustness on motor parameters variation

The robustness of the proposed system on motor parameters changes and uncertainty was tested by simulation and experimentally.

The methodology of the robustness testing was that the motor parameters were changed in the observer equation while the motor was working in open loop U/f control. The robustness was tested by comparing the computed speed with the actual speed that was measured with encoder. The parameters that were changed were rotor and stator resistances and inductances as well as the mutual inductance. The range of changes was $\pm 50\%$ for resistances and $\pm 20\%$ form inductances. Some examples are shown in Fig. 15 - Fig. 18.

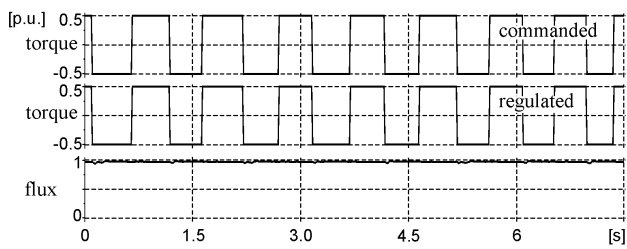


Fig. 12. Closed loop torque control - experiments.

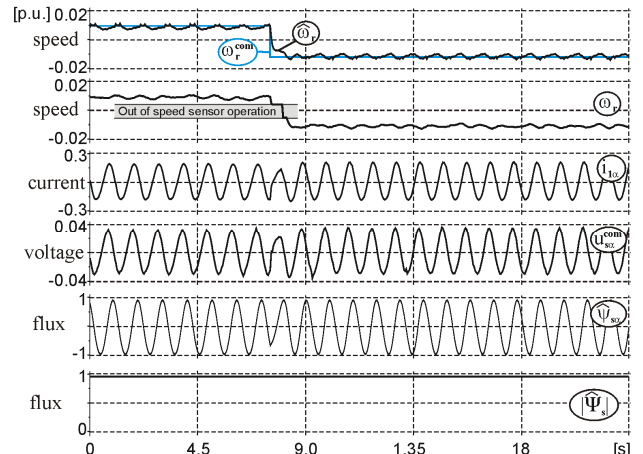


Fig. 13. Experimental results – motor reverse in low speed operation range.

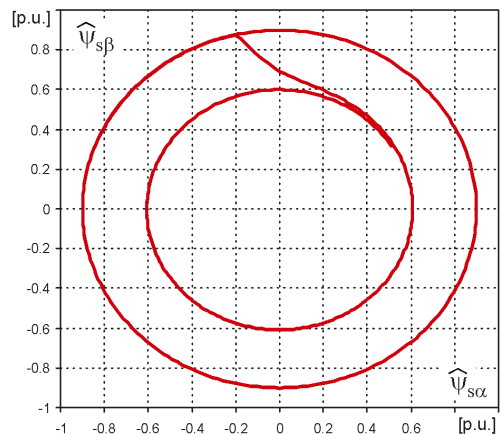


Fig. 14. Experimental results – flux control for commanded value step change $0.9 \rightarrow 0.6$ p.u.

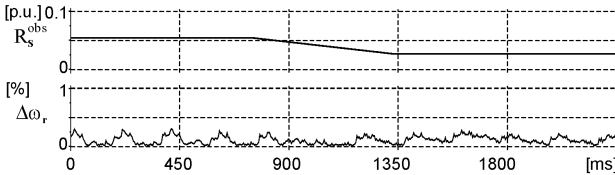


Fig.15. Speed estimation error for -50% R_s error in observer – experiment ($\omega_r=0.2$ p.u.).

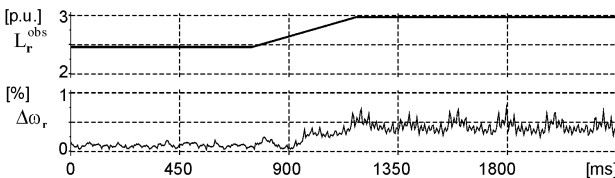


Fig.16. Speed estimation error for $+20\%$ L_r error in observer – experiment ($\omega_r=0.2$ p.u.).

It was observed that with R_r and R_s parameters changes the speed estimation error was less than 1%. However inductances could have strong influence on estimation error. It is observed for L_m in Fig. 17 or in Fig. 18.

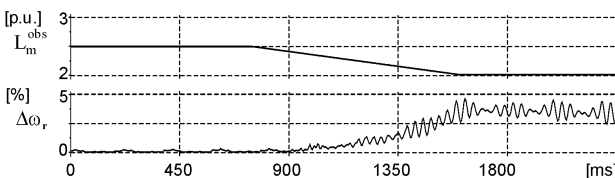


Fig.17. Speed estimation error for -20% L_m error in observer – experiment ($\omega_r=0.2$ p.u.).

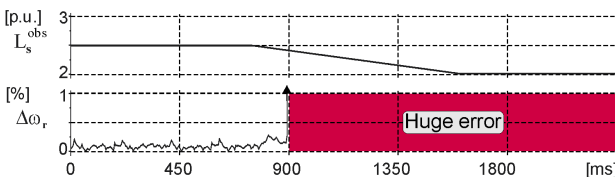


Fig.18. Speed estimation error for -20% L_m error in observer – experiment ($\omega_r=0.2$ p.u.).

The tests were done for different motor speeds and no significant differences were observed, e.g. - Fig. 19.

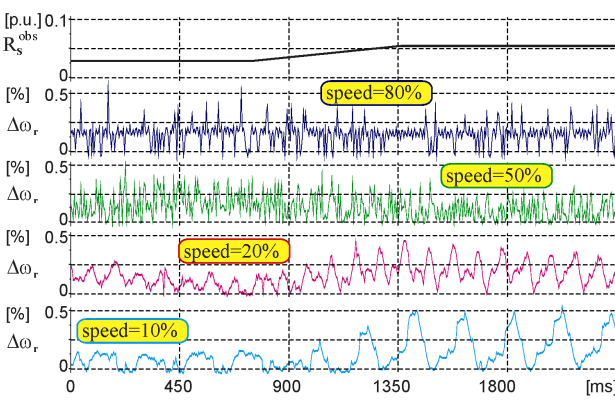


Fig.19. Speed estimation error for $+50\%$ R_s error in observer – experiment ($\omega_r=0.1 / 0.2 / 0.5 / 0.8$ p.u.).

Based on the provided experimental tests the final conclusions were collected in Table III.

TABLE III
OBSERVER ROBUSTNESS (THE LIMIT OF 1% SPEED ESTIMATION ERROR)

| Parameter [p.u.] | Upper limit | Lower limit |
|------------------|-------------|-------------|
| R_s | +50% | -50% |
| R_r | +50% | -50% |
| L_s | +20% | -4% |
| L_r | +20% | -12% |
| L_m | +7% | -10% |

Motor parameters variations have no significant influence on observer robustness. The most significant parameters are inductances especially L_m , which influence on observer operation could be noticed. However, the acceptable parameters' range variation seems to be high enough for drive correct operation. In all simulations and experiments the closed loop system was working without any on-line parameters estimation.

The next tests were done in simulation software for full sensorless system. The motor parameters used in motor model were changed. Example of the results is given in Fig. 20.

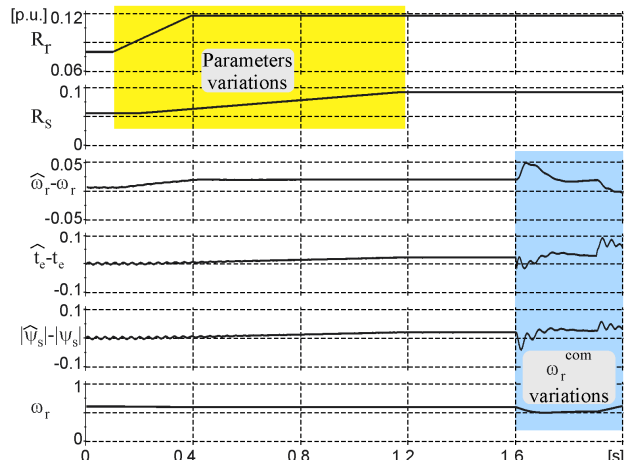


Fig. 20. Robustness test for closed loop sensorless system – simulation (R_r and R_s grows for constant speed 0.6 p.u., next the speed regulation $0.6 \rightarrow 0.5 \rightarrow 0.6$ p.u. is tested).

In Fig. 20 motor resistances R_r and R_s grow up to 150% of the nominal values. The system is working with constant speed 0.6 p.u. The accuracy of the estimated speed, torque and flux is tested. Finally, the speed regulation $0.6 \rightarrow 0.5 \rightarrow 0.6$ p.u. is tested. It is noticeable that estimation error grows for each of the variables but did not exceed 3% at steady state.

The last step was done to test the robustness of the closed loop sensorless experimental system. As in previous experiments the motor parameters used in observer calculations were changed. Example of the results is given in Fig. 21.

For the closed loop system the acceptable parameters variations coincide with given values in Table III.

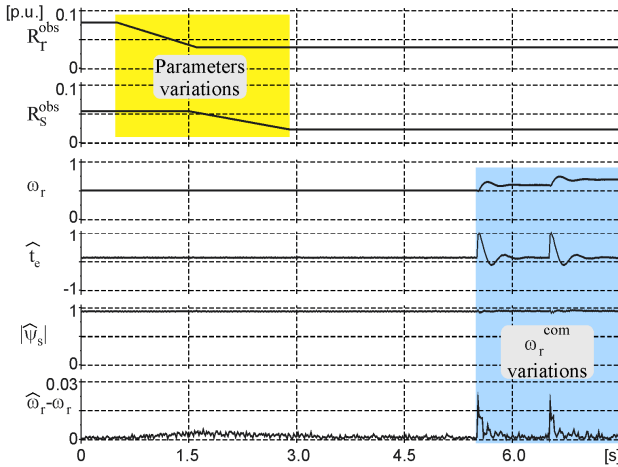


Fig. 21. Robustness test for closed loop sensorless system – experiment (R_r and R_s decreases for constant speed 0.5 p.u., next the speed regulation 0.5 → 0.6 → 0.7 p.u. is tested).

D. Diagnosis of speed sensor fault

In spite of sensorless system development a lot of drives is operating with speed senor e.g. in some rail traction drives [27] or others.

In case of motor speed sensor fault the drive can not work properly and is probably switched off immediately

To solve this problem, the motor speed calculations or estimation instead of speed measurement could be implemented. It is also possible for the presented system with observer and DTC-SVM control.

Example of that mode of operation is presented by experimental waveforms – Fig. 22.

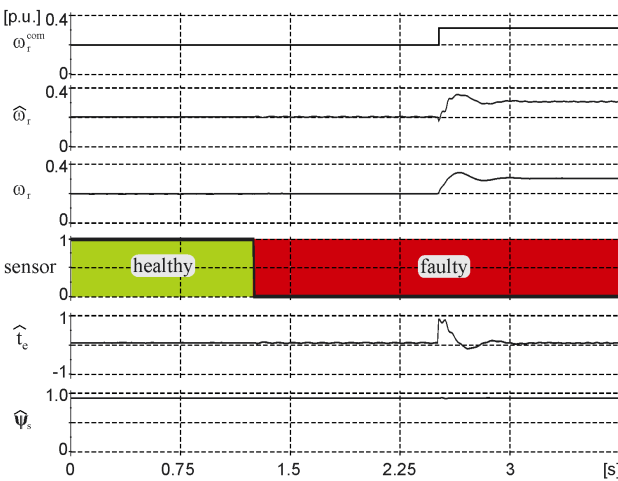


Fig. 22. Speed sensor fault identification and switch to speed sensorless control.

In Fig. 22 the speed sensor fault appeared at instant 1 s. The control system detected the fault immediately - in one step of the control calculation algorithm. Simultaneously, the whole system was switched to the speed sensorless operation mode without any noticeable disturbances. After fault detection the commanded motor speed was changed and the system has reacted correctly.

VI. CONCLUSION

Use of LC filter in electric drives requires changes in control structure – especially for speed sensorless drives. The solution of how to do that in case of DTC PWM control is proposed in the paper. It is validated by simulation and experiments.

The provided test gives result that robustness on motor parameters changes is acceptable that the real system can work without any on-line parameters algorithms.

REFERENCES

- [1] D.F. Busse, J. Erdman, R. Kerkman, D. Schlegel, G. Skibinski, "Bearing currents and their relationship to PWM drives," *IEEE Transactions on Power Electronics*, vol. 12, no 2, March 1997.
- [2] B. Muralidhara, A. Ramachandran, R. Srinivasan, M.C. Reddy, "Experimental measurement of shaft voltage and bearing current in an inverter fed three phase induction motor drive," in *Proc. 3rd International Conference on Electronics Computer Technology ICECT 2011*, 8-10 April 2011, Kanyakumari, India
- [3] P.T. Finlayson, "Output filters for PWM drives with induction motors," *IEEE Industry Applications Magazine*, vol. 4, no January/February 1998, pp. 46-52.
- [4] *IEEE recommended practices and requirements for harmonic control in electrical power systems*, IEEE standard 519, 1992.
- [5] J. Salomäki, A. Piippo, M. Hinkkanen, J. Luomi, "Sensorless vector control of PMSM drives equipped with inverter output filter," in *Proc. 32nd Annual Conference of the IEEE Industrial Electronics Society IECON 2006*, Paris, France, pp. 1059-1064.
- [6] J. Guzinski, H. Abu-Rub, "Speed sensorless control of induction motors with inverter output filter", *International Review of Electrical Engineering*, vol. 3, no. 2, April 2008, pp. 337-343.
- [7] J. Guzinski, H. Abu-Rub, "Speed sensorless asynchronous motor drive with inverter output LC filter", in *Proc. 14th International Power Electronics and Motion Control Conference EPE-PEMC 2010*, 6-8 September 2010, Ohrid, Republic of Macedonia.
- [8] M. Adamowicz, J. Guzinski, "Control of sensorless electric drive with inverter output filter," in *Proc. 4th International Symposium on Automatic Control AUTSYM 2005*, 22-23 September 2005, Wismar, Germany.
- [9] J. Guzinski, H. Abu-Rub, "Asynchronous motor nonlinear control with inverter output LC filter," in *Proc. 2nd Mediterranean Conference on Intelligent Systems and Automation CISA 2009*, 23-25 March 2009, Zarzis, Tunisia.
- [10] J. Guzinski, H. Abu-Rub, F.A. Zobaa, "Electric motor drive with inverter output filter," in *Proc. Workshop on Power Electronics for Industrial Applications and Renewable Energy Conversion PEIA 2011*, 3-4 November 2011, Doha, Qatar.
- [11] M. Depenbrock, "Direct self control of inverter-fed induction machines," *IEEE Transactions on Power Electronics*, vol. 3, no. 4, October 1988, pp. 420-429.
- [12] I. Takahashi and T. Noguchi, "A new quick-response and high efficiency control strategy of an induction machine," *IEEE Transactions on Industrial Applications*, vol. 22, September/October 1986, pp. 820-827.
- [13] G. Buja, M.P. Kazmierkowski, "Review of direct torque control of AC motors", *IEEE Transaction on Industrial Electronics*, vol. 51, no. 4, August, 2004, pp. 744-757.
- [14] E. Monmasson, A.A. Naassani, J.P. Louis, "Extension of the DTC concept," *IEEE Transactions on Industrial Electronics*, vol. 48, no. 3, June 2001, pp. 715-717.
- [15] J. Guzinski, Z. Flisikowski, "Practical application of induction motor direct torque control," in *Proc. VIII Seminar of Electric Drive and Control Systems Development*, 12-14 February 2002, Gdansk, Poland. (in polish)
- [16] M.P. Kazmierkowski, R. Krishnan, F. Blaabjerg, "Control in power electronics," Academic Press. 2002.
- [17] D. Swierczynski, P. Wojcik, M.P. Kazmierkowski, M. Janaszek, "Direct torque controlled PWM inverter fed PMSM drive for public transport," in *Proc. 10th IEEE International Workshop on Advanced Motion Control, AMC '08*, 26-28 March 2008, Trento, Italy.

- [18] P.C. Loh, M.J. Newman, D.N. Zmood, and D.G. Holmes, "A comparative analysis of multiloop voltage regulation strategies for single and three phase UPS systems," *IEEE Transactions on Power Electronics*, vol. 18, no. 5, September 2003, pp. 1176-1185.
- [19] R. Seliga, W. Koczara "Multiloop feedback control strategy in sine-wave voltage inverter for an adjustable speed cage induction motor drive system," in *Proc. European Conference on Power Electronics and Applications, EPE'2001*, 27-29 August 2001, Graz, Austria.
- [20] P.C. Loh, M.J. Newman, D.N. Zmood, and D.G. Holmes, "A comparative analysis of multiloop voltage regulation strategies for single and three phase UPS systems," *IEEE Transactions on Power Electronics*, vol. 18, no. 5, September 2003, pp. 1176-1185.
- [21] M.J. Ryan, R.D. Lorenz, "A high performance sine wave inverter controller with capacitor current feedback and Back-EMF decoupling," in *Proc 26th Annual IEEE Power Electronics Specialists Conference, PESC'95*, Atlanta, GA, USA, 18-22 June 1995, pp. 507-513.
- [22] J. Choi, B. Kim, "Improved digital control scheme of three phase UPS inverter using double control strategy," in *Proc. IEEE 12th Applied Power Electronics Conference, APEC'97*, 23-27 February 1997, Atlanta, Georgia, USA, pp. 820-824.
- [23] J. Guzinski, "Sensorless AC drive control with LC filter," in *Proc. 13th European Conference on Power Electronics and Applications, EPE'2009*, 8-10 September 2009, Barcelona, Spain.
- [24] Z. Krzeminski, "Sensorless Control of the Induction Motor Based on New Observer," in *Proc. 37th International Conference on Power Conversion and Intelligent Motion, PCIM'2000*, June 2000, Nuremberg, Germany.
- [25] H. Abu-Rub, A. Iqbal, J. Guzinski, "High performance control of ac drives with MATLAB/Simulink models," Wiley, 2012.
- [26] X. Xue, X. Xu, T. G. Habetler, and D. M. Divan, "A low cost stator flux oriented voltage source variable speed drive," in *Proc. IEEE-IAS Annual Meeting*, vol. 1, 7-12 October 1990, pp. 410-415.
- [27] J. Guzinski, H. Abu-Rub, M. Diguet, Z. Krzeminski, A. Lewicki, "Speed and Load Torque Observer Application in High-Speed Train Electric Drive," *IEEE Transactions on Industrial Electronics*, vol. 57, no. 2, February 2010, pp. 565-574.